AD NUMBER

AD874283

LIMITATION CHANGES

TO:

Approved for public release; distribution is unlimited.

FROM:

Distribution authorized to U.S. Gov't. agencies and their contractors; Critical Technology; 30 JUN 1970. Other requests shall be referred to Air Force Cambridge Research Laboratories, Attn: CROO, L. G. Hanscom Field, Bedford, MA 01730. This document contains export-controlled technical data.

AUTHORITY

AFCRL ltr, 22 Dec 1971

AFCRL-70-0394

OPTIMUM TECHNIQUES FOR MEASURING SPECTRAL, SPATIAL AND TEMPORAL DISTRIBUTION OF RADIATION

Adolf W. Lohmann
Department of Applied Physics and Information Science
University of California, San Diego
La Jolla, California 92037

Contract No. F 19628-69-C-0268
Project No. 8692

FINAL REPORT
Period Covered: May 1969 - June 1970
30 June 1970

This research was supported by the
Advanced Research Projects Agency

Prepared for
Air Force Cambridge Research Laboratories
United States Air Force
Bedford, Massachusetts 01730

MISSING PAGE
NUMBERS ARE BLANK
AND WERE NOT
FILMED

Qualified requestors may obtain additional
copies from the Defense Documentation Center.

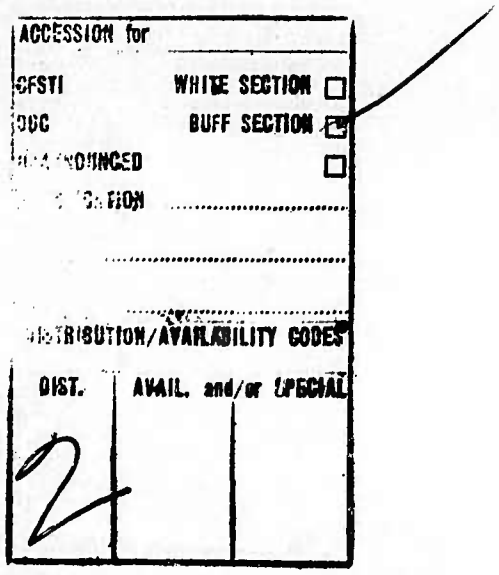

AFCRL-70-0394

OPTIMUM TECHNIQUES FOR MEASURING SPECTRAL, SPATIAL AND TEMPORAL DISTRIBUTION OF RADIATION

Adolf W. Lohmann
Department of Applied Physics and Information Science
University of California, San Diego
La Jolla, California 92037

Contract No. F 19628-69-C-0268
Project No. 8692

FINAL REPORT
Period Covered: May 1969 - June 1970
30 June 1970

Contract Monitor: Thomas P. Condron
Optical Physics Laboratory

This research was supported by the
Advanced Research Projects Agency

Prepared for
Air Force Cambridge Research Laboratories
United States Air Force
Bedford, Massachusetts 01730

ABSTRACT

It is planned to send an infrared scanner in a balloon up to high altitudes. Azimuth scanning is accomplished by the torsion of the gondola. The elevation angle of the scanning telescope is incremented stepwise after each full revolution. In this report the scanning mode is studied and improvements thereof are suggested. For a follow-up instrument it is suggested that the scanning rate should not be limited by the slow torsion. In a next approach the elevation would be scanned fast compared to the torsion. Ultimately a "multiplex scanner" should look at many directions simultaneously. The principle of a multiplex scanner is outlined.

Table of Contents

Summary

The general task is to measure from a balloon the infrared radiation S as a function of the direction it comes from, as a function of time, and for four (or six) bands of wave-numbers. The project consists of three parts:
A. Definition of the optimum scanning mode for the now existing LMSC instrument;
B. Design considerations for a future instrument;
C. Development of the software for the evaluation of data to be gathered by the existing instrument.

Part A: A scanning strategy for the existing instrument is outlined in §§1-6. Improvements of the scanning mode are suggested in §7. Even if feasible most of these suggestions are probably too late for the existing instruments. Hence the corresponding section of §7 belongs actually to Part B.

Part B: In the long range the rate of data recording should not be limited by the slow torsion of the balloon, which provides the scan movement for the azimuth angle α. A preliminary solution is proposed in §7.1.4. A long-range attempt for increasing the data recording rate is based on the concept of "Fellgett's multiplex advantage". The principle of a "multiplex scanner" is outlined in §9.

Part C: The aim is to provide a mathematical method for processing the received raw data to convert them into the best possible "image" of the sky. After describing the data flow (§10, 11, 12) a linear filter approach for image restoration is presented (§13). Under special circumstances the handicap of "dilute β-scanning" (§12) can be overcome by changing the receiver configuration and by incorporating a nonlinear scheme into the digital image restoration procedure.

§1. The Objective

The goal is to measure infrared radiation (λ = 8-12μm). The measuring instruemtn will be carried by a balloon up to a height of about 30 km. The instrument consists essentially of a telescope, a point-receiver in a fixed position of the image plane, and a recorder. The torsion oscillation of the balloon gondola will swing the telescope around, such scanning the azimuth angle α. (For details about nomenclature see §2.) The vertical direction of the telescope can be varied under remote control, such pointing at different elevation angles β on the sky. A filter wheel, also under remote control, contains various color and neutral density filters.

The objective is to devise a strategy for varying the elevation, the filter wheel and other instrumental parameters which can be optimized. After establishing the nomenclature (§2) we will describe the relevant features of the instrument (§3). Next we will choose a suitable coordinate system (§4). Then we can describe the scanning strategy (§5) together with some calibration and housekeeping procedures. In §6 we will discuss the choice of the chopper frequency. In §7 we will suggest some modifications of the scanning strategy, aimed at improving the efficiency and at concentrating on the most interesting data. §8 contains some systems considerations, and §9 is devoted to the "multiplex scanner".

The rest of this report is devoted to digital image restoration. First we describe in mathematical terms the signal flow from sky to tape (§10). The following features will be taken into account: color filters, neutral density filters, chopper, lens system, receiver size, receiver noise, electrical filtering. Next (§11) the influence of the neutral density filters will be considered more closely. Since the step $\Delta\beta$ in elevation between subsequent scanning cycles is much larger than the resolution $\delta\beta$ the recorded signal will be somewhat ambiguous, which is discussed in §12. The noise which is added to the signal in the receiver can be suppressed partially by subjecting the recorded data to a digital filtering process, which is a generalization of the Wiener filter (§13). Finally we consider means to overcome the dilute β-scanning (§12) without the need to change the scanning mode of the first-generation instrument. This method will work if all object details (or at least most of the interesting ones) are points. The implementation of this scheme requires a minor modification of the receiver and an elaboration of the digital image restoration method.

§2. Nomenclature

$S(\alpha, \beta, \sigma, t)$: radiation coming from the angular intervals $(\alpha, \alpha + d\alpha)$, $(\beta, \beta + d\beta)$ in the spectral interval $(\sigma, \sigma + d\sigma)$ during the time interval $(t, t + dt)$.

t: time.

λ: wavelength

$\sigma = 1/\lambda$: wave number.

α: azimuth angle, projected into horizontal plane.

$\alpha = 0$: magnetic north direction.

$1° = \pi/180$ rad = 17.43 mrad; 1 mrad = 0.0573 deg.

$\pi/2 - \beta$ (in rad): elevation.

$\beta = 0$: zenith.

$\beta = \pi/2$ rad: equatorial or horizontal plane.

$\alpha = \alpha_M \sin\{2\pi\Omega(t - t_0)\}$: torsion of gondola

$1/\Omega$: full period of torsion oscillation.

α_M: angular amplitude of torsion; maybe $> 2\pi$.

$\omega = 2\pi\, \alpha_M \Omega \cos\{2\pi\Omega(t - t_0)\}$: angular velocity of gondola.

ν_t: time frequency.

ν_c: chopper modulation frequency.

x_M: position on magnetic tape.

δx_M: resolution of the tape.

L: total length of the tape.

v: tape velocity.

ν_M: bandwidth of magnetic tape.

ν_T: bandwidth of telemetry system.

index E: earth related coordinate system.

index S: sky related coordinate system.

index G: gondola related coordinate system.

$\beta_s(t)$: swiveling of the gondola's vertical axis.

x', y': orthogonal coordinates in the image plane of the telescope; the x'-axis is horizontal.

f: focal length of the first lens in the telescope.

$F_m(\sigma)$: spectral filter functions, m = 1 . . . 4, or 1 . . . 6.

S_m: spectral component of S, as selected by F_m.

z-axis: gondola axis $\beta = 0$.

x-axis: towards magnetic north.

y-axis: perpendicular to x- and z-axis.

$\Delta\beta$: elevation steps.

$\delta\beta$: resolution in elevation

T_j: transmittance of the j-th neutral density filter.

$S_{mj}(\alpha, \beta)$: $= S_m T_j$.

M(x', y'): point spread function of the lens system.

$\tilde{M}(\nu, \mu)$: optical transfer function of the lens system.

R(x', y'): spatial distribution of the receiver.

$P(\alpha'\sin\beta_1, \beta')$: angular spread function of the telescope.

$S_E(\alpha)$: one-dimensional equivalent object radiation.

$\tilde{G}(\nu_t)$: transfer function of the electrical system.

$U_R(t)$: signal recorded on tape

$\tilde{D}(\nu_t)$: digital filter function for noise suppression.

§3. The Parameters of the Instrument

The telescope is carried by a balloon to an altitude of about 30 km., where it will stay for about four hours. The elevation of the telescope can be changed in flight. In vertical position ($\beta = 0$) the telescope would point towards the balloon. Hence nothing is lost if a heat source for σ-calibration is mounted in that direction. The highest elevation (smallest angle β) accessible for radiation measurements of the sky is called β_0. The instrument range of β extends to the equatorial plane ($\beta = \pi/2$; also called parahorizon) and beyond to the earth horizon at about $\beta_E = \pi/2 + 1/10$ (for an altitude of 30 km). There is danger that the gondola might "swivel", causing β-oscillation of the telescope's direction. Nothing definite seems to be known about the amplitude and frequency of these β-oscillations.

The azimuth of the telescope is fixed with respect to the gondola. Due to the torsion oscillation of the gondola the telescope will aim at

$$\alpha(t) = \alpha_M \sin\{2\pi\Omega((t - t_0))\}. \qquad (3.1)$$

The torsion amplitude α_M is expected to be several revolutions, say $\alpha_M \sim 6\pi$. It can be predicted only roughly before the flight. Also the torsion frequency Ω or its inverse, the torsion period $1/\Omega$ cannot be exactly determined from preflight measurements. But the lower bounds for α_M and Ω should be known before the flight, because other instrumental parameters have to be adjusted accordingly. To get an idea of the orders of magnitude we start from the assumption that the average of azimuthal velocity $\dot{\alpha} = \omega$ might be π rad/min = 1/20 rad/sec. Since $\|\omega\|_{AVERAGE}$ is $4\alpha_M\Omega$ we get with $\alpha_M = 6\pi$ rad now $1/\Omega = 1500$ sec ≈ 24 min.

The telescope has an aperture diameter of 5 inches $\approx$ 125 mm. For the longest wavelength (12μm) this results in a theoretical angular resolution of 10^{-4} rad. Considering the difficulties of designing the infrared lens system consisting of so few elements it would not be surprising to measure a practical resolution ten times larger, say $\delta\alpha = 10^{-3}$ rad = 1 mrad. Of course the modulation transfer function (MTF) would describe more completely the influence of the lens system. In the image plane of the telescope are four (not only one) receivers horizontally side-by-side. Two receivers have a size of 1×1 mrad^2, and the others 2×2 mrad^2. Their angular distances are each 5 mrad from center to center. The corresponding length measures follow from the focal length f = 9.5 inch $\approx$ 240 mm of the primary lens. In the intermediate image plane is a filter wheel, which contains three neutral density filters of transmittances 10^{-1}, 10^{-2}, 10^{-3}, and four color filters with spectral ranges 8.3-13mμ, 9-10.5mμ, 10.5-11.5mμ, and 11.5-12mμ. Two additional color filters (8.3-9mμ, 12-13mμ) are available as standbys. The spectral transmittance of the lens system and the spectral sensitivity of the receivers are known to be flat within 15%. The temporal response of the receivers is characterized by a time constant of 2 msec. The noise is probably caused mainly by the receiver independently of the incoming radiation. The noise spectrum decreases somehow with increasing temporal frequency ν. A chopper in the intermediate image plane has N spikes and rotates M times per second. Hence the radiation is modulated by $\nu_c = NM$, which is planned to be 200 HZ.

The signals as picked up by the four receivers are recorded on a multi-track magnetic tape, which moves with velocity v. The resolution length δx and the total length L of the tape are significant parameters. The bandwidth ν_M of the tape recorder is connected with δx and v by $\nu_M = v/\delta x$. The dynamic range of the tape is also a relevant parameter. Possibly the receiver signals will not be recorded on tape but transmitted immediately to an earth-based recorder. In that case the bandwidth ν_T of the telemetry system is important.

§4. Choice of a Coordinate System

The choice depends on what is meaningful for describing the "object", what can be calibrated, and what is convenient for data processing. Basically one could choose the sky, the earth, the gondola or the balloon as the frame of reference. Since the earth rotates with an angular velocity of 2π rad/day = 4 mrad/min the stars will not be completely stationary objects in an earth-related system, which speaks against the earth frame of reference. Nevertheless we prefer the earth-related coordinate system because it can be calibrated most conveniently. Gravity provides a basis for definite the zenith at $\beta = 0$, and the earth's magnetic field can serve to calibrate the azimuth angle $\alpha = 0$. The earth system differs from the gondola system due to the torsion and due to swiveling:

$$\alpha_E - \alpha_G = \alpha_M \sin\{2\pi\Omega(t - t_0)\}; \tag{4.1}$$

$$\beta_E - \beta_G = \beta_s(t). \tag{4.2}$$

The center ($x' = 0$, $y' = 0$) of the telescopes image plane corresponds to the point α, β on the sky: $\alpha_M \sin\{2\pi\Omega(t - t_0)\}$; $\beta_s(t)$. A shift by dx', dy' in the image plane means a shift in angular coordinates by

$$d\alpha = \sin\beta\, dx'/f; \qquad d\beta = dy'/f. \tag{4.3}$$

The various spectral filter functions are called $F_m(\sigma)$; $m = 1, 2, 3, 4$. They are meant to describe the filter transmittance, but also the lens transmittance and the receiver sensitivity. We will call S_m the spectral components of the object,

$$S_m(\alpha, \beta, t) = \int S(\alpha, \beta, \sigma, t)\, F_m(\sigma)\, d\sigma. \tag{4.4}$$

§5. Calibrations, Scanning Mode, Housekeeping

Before the flight the following quantities should be measured: Transmittance of neutral density filters, spectral transmittance of neutral density filters, spectral transmittance of color filters and lens system, MTF of the lens system in connection with various color filters, flare rejection rate, spectral sensitivity of receiver, dark current of receiver, time-constant of

receiver, non-linear response of receiver, linearity and frequency filter of amplifiers, linearity and frequency response of tape, chopper frequency ν_c.

The parameters α_M, Ω, β_S, which relate to the torsion and swiveling of the gondola should be estimated based on an experiment. A method for choosing α_M deliberately should be studied. That is, the gondola might be pre-twisted and hooked before take-off, and released for torsion oscillation when at operational altitude. The time it takes to perform a σ-calibration under remote control should be measured in the laboratory.

In flight the instrument should be checked out by performing at first a σ-calibration. For this purpose the telescope has to be pointed at the reference heat source at $\beta = 0$. Next it will be checked if the azimuthal velocity ω is large enough. For this purpose the elevation is aimed at the earth horizon, where many radiation sources can be expected. The electrical signals from the four receivers are added. The four signals are roughly alike, but delayed by 5 mrad/ω, which is the time it takes for an object point to wander from one receiver to the next one. A coarse electronic filter bank will find out the resonance frequency ω/5 mrad in the combined signal, from which ω can be derived. If this method for sensing ω is not feasible ω should be measured by some other method, perhaps based on centrifugal forces. At any rate it would be a waste of magnetic tape, if the measurement would begin at a very low torsion-angular velocity ω.

If ω is large enough, say at least 30 mrad/sec, the measurement can begin. The telescope is elevated to the steepest angle β_0; the four receiver amplifiers are disconnected; the tape is started; the starting time is recorded; the starting angle with respect to a magnetometer is recorded for housekeeping purposes; the highest transmittance neutral density filter is inserted together with the color filter m = 1, which covers the whole spectral range. During the first α-cycle the output signal of the amplifiers is checked to see if it exceeds a critical level which corresponds to the upper end of the dynamic range of the tape recorder. If this level was exceeded, the next denser neutral density filter is inserted for the next α-cycle. Elevation β_0 and color filter F_1 remain the same. If again the critical level is exceeded the next neutral density filter is inserted for the next α-cycle. If now an α-cycle is completed without exceeding the critical level color filter F_2 is inserted and the n.d. filter is exchanged for the next higher transmittance, because F_1 lets pass much more energy than any of the other filters F_2, F_3, F_4. The latter three are roughly alike in that respect. Once F_4 has been run through at elevation β_0 the elevation will be changed $\beta_0 + 1/10 = \beta_1$. Now again a similar cycle begins. In order to save time each filter F_m will be run in connection with the same n.d. filter as was proper at elevation β_0. This guess might not always be adequate. The criterion for choosing the next denser filter would be as before. On the other hand, if the amplifier output never comes up to the critical level the α-cycle will be rerun with the next more transparent n.d. Filter. For "closing" the program a run with the densest of all n.d. filters must be declared as successful even if the amplifier did exceed the critical level.

The increases in β-steps by 1/10 rad will go on till β has reached an elevation where the telescope aims at the earth. That β-position will not be

executed; rather, the command will be: return to and start all over. A series of cycles over all β-positions takes much longer time than a half-period 1/2 Ω of the torsion oscillation. The measurement cycle will be interrupted when the angular velocity ω falls below critical level. During the off-time (while $|\omega| < \omega_c$) the σ-calibration is repeated. The duration of the "off-time" depends on α_M, Ω and ω_c. Giving these parameters, or at least conservative estimates, allows specifying the time available for the σ-calibration and other instrumental check-ups.

A housekeeping track on the tape shall record clock-signals, α-markings from the magnetometer and records of all events like changes of filters, elevation jumps, and calibration results.

§6. Choice of the Chopper Frequency

It is advantageous to chop the radiation periodically, because a.c. amplifiers are easier to operate than d.c. amplifiers. Also the signal-to-noise ratios might be influenced favorably, as we will discuss after establishing two boundaries for the chopper frequency ν_c. The chopper frequency ν_c is the product of the revolutions per unit time of the chopper wheel and the number of angular periods on the rotating chopper mask.

ν_c has to be high enough so that the signal is still recognizable after chopping. The finest periodic object structure which can be resolved has a period of δα rad. When scanned by the telescope which spins with angular velocity ω rad/sec this periodic object structure will generate in the receiver a periodic signal with a time frequency $\omega/\delta\alpha$. The chopper frequency ν_c which acts like a modulation carrier frequency has to be twice as high as the highest object frequency, hence

$$\nu_c > 2\omega/\delta\alpha. \tag{6.1}$$

In the worst case ω will be $\omega = \omega_{MAX} = 2\pi\,\alpha_M$. Assuming $\delta\alpha = 10^{-3}$ rad, $\alpha_M = 6\pi$ rad, $1/\Omega = 1500$ sec, we get

$$\nu_c > 4\pi\,\alpha_M\,\Omega/\delta\alpha = 160 \text{ HZ}. \tag{6.2}$$

On the other hand the chopper frequency should not be unnecessarily large. Otherwise the bandwidth of the tape might not be sufficient. The upper sideband of the modulated signal has a frequency of $\nu_c + \omega/\delta\alpha$ (c.f. equ. 6.1). The highest possible frequency ν_M to be recorded on the tape depends on the tape speed v and the tape resolution δx like $\nu_M = v/\delta x$. Hence we must request

$$\nu_c + \omega/\delta\alpha < \nu_M = v/\delta x. \tag{6.3}$$

Since we want the tape speed to be as low as possible we select the smallest possible chopper frequency ν_c (equ. 6.1 and 6.2),

$$3\omega/\delta\alpha < v/\delta x. \tag{6.4}$$

Making the same assumptions as for equ. (6.2), and also $\delta x = 25m$ it follows as minimal tape velocity

$$v > 3\omega_{MAX}\, \delta x/\delta\alpha = 6mm/sec. \tag{6.5}$$

Over a period of 4 hours = 14,400 seconds this requires a tape length of

$$L = v \cdot 14{,}400 = 86.4\ m. \tag{6.7}$$

Now let us discuss how the signal-to-noise situation influences the choice of the chopper frequency ν_c. Although the specific assumptions are rather vague this consideration is nevertheless meaningful in principle. The additive noise spectrum might be proportional to $1/\nu$, and the sensitivity of the receiver might vary like $1/[1 + (\nu/\nu_R)^2]$. Hence the signal-to-noise ratio at the chopper frequency is

$$\nu_c/[1 + (\nu_c/\nu_R)^2]. \tag{6.8}$$

It has a maximum if ν_c is chosen to be equal to ν_R, at which frequency the receiver sensitivity has dropped to 1/2 of its d.c. maximum. Probably ν_R, which is roughly the inverse of the receiver time constant, will be at least in the KHZ region, so it is not sensible to bring up the chopper frequency to the same level. Yet equ. (6.8) confirms at least qualitatively that it is better to chop than to work with d.c. signals.

§7. Improved Scanning Mode

The scanning mode described in §5 is based on the discussions with AFCRL and LMSC representatives (August 1969). That scanning mode should be compatible with the hardware design. However, several aspects could be improved with a moderate amount of hardware changes. The improvements aim mainly at better light efficiency and matching the bandwidths of the various components.

§7.1 (α, β) Scanning Mode

Employing the scanning mode as described in §5, it takes a fairly long time to complete a full (α, β) cycle. It is mainly the angular velocity ω of the gondola which slows down the data rate. The electronics and the tape recorder could digest much higher data rates. Avoiding this mismatch and introducing some conveniences are the aims of this section.

§7.1.1 β-Interlace

The β-steps were designed to be 0.1 rad, while the β-resolution is perhaps 100 times finer. This leaves fairly wide β-zones unobserved. To eliminate this handicap at least partially, the first (α, β) cycle might cover

rings β_0, $\beta_0 + 0.1$. $\beta_0 + 0.2$, etc. the second (α, β) cycle would be interlaced like $\beta_0 + 0.01$, $\beta_0 + 0.11$, $\beta_0 + 0.21$, etc., and the third cycle $\beta_0 + 0.02$, $\beta_0 + 0.12$, etc. This numerical example is adequate, if total time (4 hours) would cover ten (α, β) cycles.

§7.1.2 Concentrating on the Horizon Belt

The most interesting details are probably to be found around the para-horizon $\beta = \pi/2 \pm 1/10$. Hence within this belt the β increment should be finer than at the higher elevations.

§7.1.3 Continuous β-Increase

At the moment when β is increased by a discrete amount (like 0.1) some data might be lost, because the telescope might vibrate for a short while. Hence a constant $d\beta/dt$ might be better. If an increment of $\delta\beta$ per revolution is wanted $d\beta/dt$ should obey

$$(d\beta/dt)/(d\alpha/dt) = \delta\beta/2\pi;\ d\alpha/dt = \omega. \qquad (7.1)$$

This implies that $\omega = \omega(t)$ must be known. Knowledge of ω can be gained in several ways: t(the clock) and $\alpha(t)$ are recorded anyway for housekeeping purposes. ω can be derived from α and t. Or t and $\omega(t)$ are constantly measured. Or, since the time t is not interesting explicitly it would be good enough to monitor α and $\omega(\alpha)$. At any rate $(d\beta/dt)/(d\alpha/dt)$ would be $<< 1$, because a high $d\beta/dt$ of the telescope would probably cause mechanical problems.

§7.1.4 Vertical Telescope and Rotating Mirror

So far the data rate depends mainly on the angular velocity ω of the torsion and on the angular resolution $\delta\alpha$. Pro unit time the telescope will point at $\omega/\delta\alpha$ different resolution elements. With $\omega = \pi$ rad/min = 1/20 rad/sec and $\delta\alpha$ = 1/1000 rad this results in 50 data per second. Such a low data rate is certainly far below what can be handled conveniently by the receivers, the electronics and the tape recorder. This data rate is probably also far below a level where photon noise would be severe. Hence we suggest a different (α, β) scanning mode with a much higher data rate, which can be adjusted freely.

The telescope is fixed in the gondola. It points vertically to the zenith ($\beta = 0$). A prismatic body with quadratic or polygon cross section has mirror surfaces. This multi-mirror is placed on top of the telescope where it rotates around its axis in horizontal position. A horizontal hollow cylinder in front of the rotating mirror selects coarsely the β-range of interest. The β-scan rate $d\beta/dt$ is two times the angular velocity of the spinning mirror. The β-scan rate can now be much larger than the α-scan rate ω. The α-steps depend on the ratio of ω to $d\beta/dt$, and of the number of facets on the spinning mirror. This number has to be matched to the β-belt of interest, which is preselected by the hollow cylinder. The four receiver elements may be lined

up in parallel to the axis of the spinning mirror. Hence they scan at different α-positions, avoiding redundancy of the four receiver signals as in the origianl setup. Originally, the reason for letting the four receivers scan through the (α, β) domain at exactly the same paths was the possibility for detecting fast temporal changes of the object $S(\alpha, \beta, \sigma, t)$. This reason is not very valid anymore, because with the vertical telescope a full (α, β) cycle will be finished much faster, perhaps a hundred times.

§7.1.5 Monitoring the Swiveling of the Gondola

Instruments for measuring the swiveling $\beta_S(t)$ of the gondola are probably available in the aircraft industry. But it could be that $\beta_S(t)$ is difficult to measure because β_S is very small (hopefully) and very slow. In that case a simple hydrodynamic instrument might be desirable. A tube system could form a triangular star as large as the gondola floor. The three spikes are slightly bent upwards. The tube consists of electrically insulating material and is partially filled with a conductive fluid. Pairs of electrodes are at the ends of the three spikes. Whenever a spike tilts down the fluid will close the electrical connection in that spike. Monitoring the on-off events might be sufficient enough for deducing the swiveling of the gondola.

§7.2 Modifications of the Chopper and Filter Wheel

The reasons for modifying the chopper and filter wheel are two-fold: some objects on the sky might reveal a clue about their identity if their spectral characteristics are known, for example a quantity like $(\partial S/\partial\sigma)/S_{AVERAGE}$. To get this quantity we might want to measure the spectral components S_1, S_2, S_3, S_4 in rapid sequence before (α, β) have changed markedly. Furthermore the efficiency of collecting radiative energy and data can be increased by making the scanning mode more flexible, instead of designing it rigidly on the basis of worst-case considerations.

§7.2.1 Instant Adaption of Neutral Density Filters

So far (5) we had planned to change neutral density filters only after full α-cycles. That simple strategy might require that the same α-cycle be repeated several times when n.d. filters are required. This waste of time can be avoided if the n.d. filters change instantly whenever certain clipping levels are reached. The hardware to do this can be designed as in a modern recording photometer.

§7.2.2 High-Speed σ-Scanning

Instead of exchanging color filters stepwise after full α-cycles one might place little pieces of color filter in sector-form on the chopper wheel. Remember, the chopper wheel is imaged 1:1 onto the receiver elements. For simplying the argument let's say the filters used so far have each a spectral

passband of 1mμ width, covering the ranges (8-9mμ), 9-10mμ), (10-11mμ) and (11-12mμ). It would be better to take a set of complementary filters instead: (9-12mμ), (8-9 + 10-12mμ), (8-10 + 11-12mμ), (8-11mμ). This does not improve the color discrimination, but it increases the average-color signal by a factor three, which is desirable if the scanning speed is energy-limited.

§7.2.3 Angular Color Wedge Filters

Color wedge filters (OCLI) are based on the fact that (in good approximation) the σ-transmittance curve of a multilayer film will be stretched along the σ-axis by a factor M, if all layer thicknesses are reduced by a factor 1/M. Angular color wedges are produced by evaporating onto a substrata which spins with variable velocity. A thin sector slit exposes only a small portion at a time for the deposition of a layer. Hence thickness and σ will vary with the angular position φ on the angular color filter.

The angular color wedge might be easier to put onto the chopper wheel than sector pieces of interference film. Also a continuous σ-variation is probably more convenient than stepwise σ-changes for data evaluation. It should be possible also to produce an angular color wedge with a "complementary passband" as described in §7.2.2.

§7.2.4 Angular Color Wedge for Fourier Spectrometry

If later the number of resolvable spectral elements should be larger than four (as now) the multiplex advantage of Fourier spectrometry might be exploited in the following way: First a fixed pre-filter selects the total range (8-12mμ). Next an angular wedge filter with transmittance like $1 + \cos(b\ \sigma\ \varphi)$ covers the receivers and spins ($\varphi \rightarrow \dot{\varphi}t$). The σ-integrating properties of the receiver produce the Fourier transform of the source $S(\sigma)$ at that particular point (α, β). To say the same thing in another way, the spectral transmittance of the spinning filter is such that each spectral component σ is chopped by its own specific chopper frequency $\nu_c(\sigma)$. Effectively the same can be achieved if a linear color wedge of the cosine-variety is placed on top of a slit receiver. A sector star with its number of spikes increasing in proportion to the radium spins on top of the slit receiver such that each point has its own specific chopper frequency.

§7.3 Economy Considerations for Receivers, Amplifiers and Recorder

As pointed out earlier, the data rate in the receiver is so low that probably the bandwidths of the four receivers, the four amplifiers and the tape recorder are not fully utilized. The setup with the vertical telescope (§7.1.4) was already a step in the right direction towards more economical bandwidth matching.

§7.3.1 Only One Amplifier

To have four amplifiers in parallel is not only four times as expensive, it also requires balancing these amplifiers, for otherwise one could not compare the outputs from different amplifiers. Since the bandwidth of an amplifier can be easily much wider than the temporal spectrum produced by scanning and chopping of the signal one can assign different carrier frequencies to different object parameters (time frequency multiplexing). One example of this category is the Fourier spectrometer (§7.2.4). Other examples would require other chopper disk configurations.

§7.3.2 Fresnel-Encoding Receiver

The receiver may consist of a narrow long stripe which is covered by an absorbing pattern like a sector of a Fresnel zone plate. Since there is only one receiver only one amplifier is needed. The scanning direction is now along the receiver axis such that each object point creates a temporal "chirp" or FM signal. This recording method compares to a point-receiver method like Girard's grille spectrometer compares to a slit spectrometer. The decoding of the chirp-convolved signal can be done by a digital computer, by an electronic correlator or by an optical analog computer, which is nothing but a holographic reconstruction setup. Remember, a Fresnel-hologram is the convolution of object and Fresnel pattern. Image reconstruction means to undo the Fresnel convolution. That is what we have to do with a photographically recorded amplifier output. Since this artificial hologram has been convolved with a one-dimensional Fresnel pattern, a lens system which includes at least one cylinder lens is needed, as it is well known from one-dimensional holography.

§7.3.3 Use of an A/D Converter

An A/D converter behind the amplifier has several advantages. In this project it is probably most important that non-linear distortions of any analog recording medium are circumvented. An A/D converter would also be natural if the data shall be transmitted in PCM. The question might arise if temporal modulation by a chopper is meaningful if an A/D converter follows. The answer is probably "yes", because the signal frequencies should be shifted away from the noisy frequency region around d.c. Finally an A/D converter would be natural, if the system shall communicate with a digital computer.

§7.3.4 Variable Speeds of Chopper and Tape Recorder

If the data rate is proportional to angular torsion frequency ω, the chopper might slow down if the torsion gets slower: $\nu_C \propto \omega$. Since chopping is something like sampling, it means that the chopper sampling rate is always sufficiently high to match the data scan rate. But if the chopper frequency varies proportionally to ω, the tape velocity ν_T might do the same in order not to waste any tape. A tape recorder velocity proportional to $\omega = d\alpha/dt$ would

be convenient because now the length coordinate x on the tape is directly proportional to the angular coordinate α of the object $S(\alpha)$.

§8 Systems Considerations

§8.1 Systems Layout

During the actual balloon experiment various types of data will flow between the various components as depicted in figure 1. The abbreviations in this figure are explained in table 1, "List of Components". There are the data signals gathered by the LMSC instrument from where they are sent to an A/D converter. Then there are several command signals which initiate actions like removing the cap from the telescope. Furthermore there are housekeeping signals, which record angular and time coordinates as well as the state of the instrument (filter wheel, etc.). The purpose of devising figure 1 was to get a feel for the total system and to make sure that enough housekeeping signals are recorded so that the data signals can be properly identified.

§8.2 Economy-Reliability Considerations

If one were sure what kind of signal data to expect one could send a control unit with a fixed command program along in the balloon. In that case no telemetry link from ground to balloon would be needed. If the recovery of the balloon were certain no telemetry link would be needed from "up" to "down". However, a suitable recorder must be on board. The need for real-time operation, the reliability of various components, space and weight of the components in the balloon and price are other factors which influence the strategy of the experiment.

There are nine conceivable options depending on whether a control unit is up and/or down and whether a storage unit is required up and/or down. These nine options together with the equipment requirements are listed in table 2. The ninth option is most expensive but also most reliable and flexible. AFCRL chose this option in order to be best prepared for many unforseeable situations during the first experiment.

§8.3 Test Procedures

Before the actual experiment the instrument has to be tested in various ways. AFCRL has considered already the radiometric test procedures concerning sensitivity, dynamic range, filters and amplifier gains. These radiometric tests must be coordinated with resolution tests, which take into account the modulation transfer function of the telescope and temporal effects such as chopper frequency and electronic time constants.

§8.4 Remaining Problems to be Covered in §§10-13.

A mathematical formulation of the flow of signal data has to be developed taking into account the modulation transfer function (MTF) of the telescope and the frequency responses of the electronic components. Based on this mathematical model a computer program has to be devised which allows recovery of the original data by removing the influence of the MTF, etc. as much as is meaningful under the signal-to-noise circumstances.

Table 1

List of Components

Cap	LMSC Telescope	CAP
Elevation drive β	LMSC Telescope	ELEV
Chopper	LMSC Telescope	CHOP
Filter Wheel	LMSC Telescope	FILT
Magnetometometer		MAGN α
$d\alpha/dt$ (d/dt of magnetometer or centrifugal)		$d\alpha/dt$
Clock t		CLOCK
Altimeter		ALTI
Telem. Recv. and Amplif.		TELE-R
De-Multiplexer		DE-MLPX
On Board Control Unit		CONTROL
Amflif., A/D		A/D
8-Track Store		8-TRACK
Multiplexer		MLPX
Amplif. and Telem. Emitter		TELE-E
Swivel Monitor $\beta_s(+)$		SWIV
4 Radiation Receivers		4 RAD RCV
D/A or A/D Converter		D/A or A/D
Calibration Source		CAL
Emitter		EMIT
D/A and Multiplexer		D/A & MLPX
Computer		COMP
Receiver		RECEIV
Store		STORE

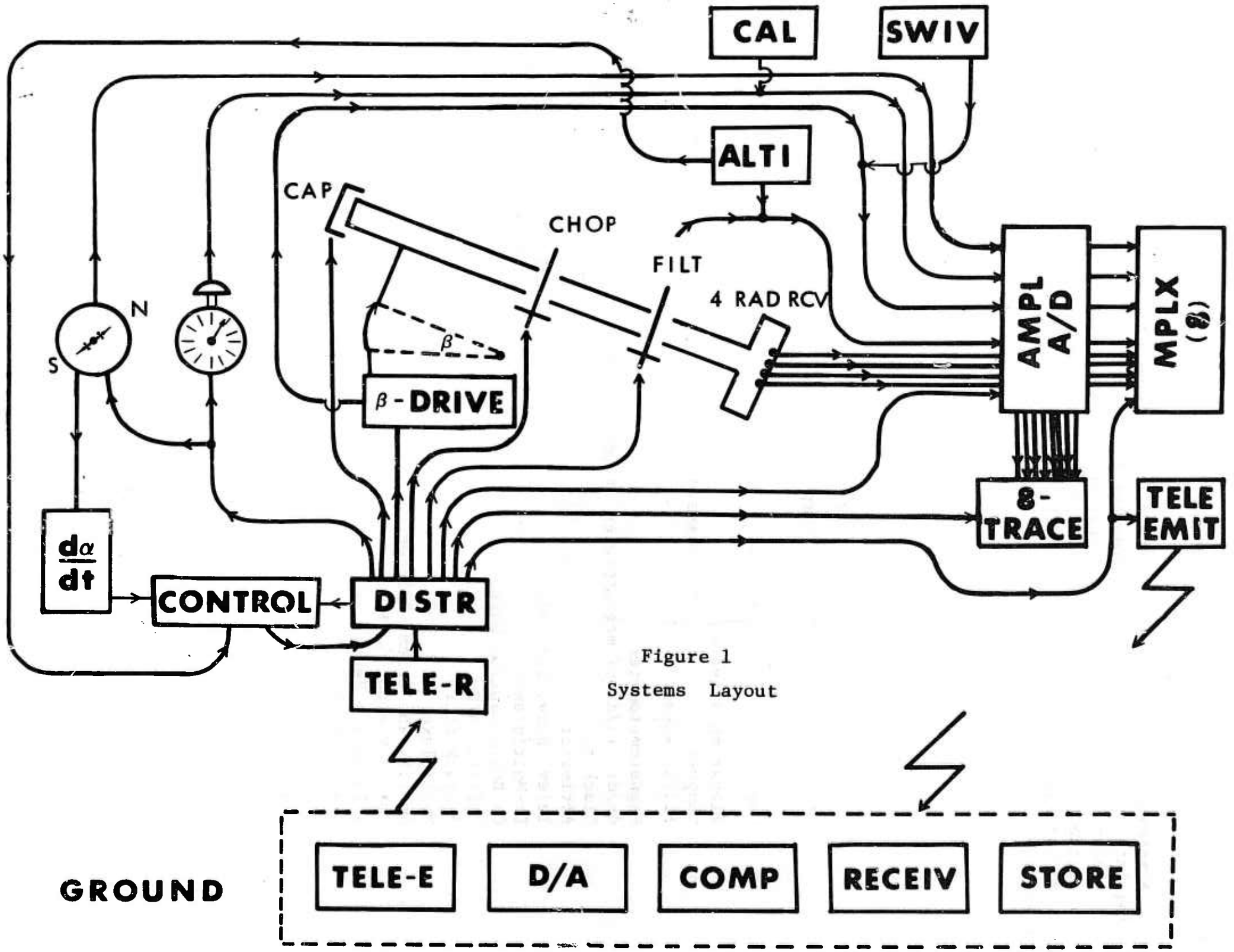

Figure 1

Systems Layout

Table 2

Nine Instrumental Options

FUNCTION	1	2	3	4	5	6	7	8	9
Up	C S	C	C	S			S		
Down		S		C	C S	C		S	
Both			S			S	C	C	C S
EQUIPMENT	**1**	**2**	**3**	**4**	**5**	**6**	**7**	**8**	**9**
Up	C S	C E S R	C S E S R	S R C E	E R C S E R	S E R C S E R	C S R C E	C E R C S E R	C S E R C S E R
Down									

§9 A Multiplex Scanner Based on the Talbot Effect

In 1836 F. Talbot described an effect which was explained about fifty years later by Lord Rayleigh. Today this effect is known by the names "Fourier images" (Cowley and Moodie, Proc. Phys. Soc. B70, 486, 1957; B76, 378, 1960) or "self-imaging" (Montgomery, J. Opt. Soc. Am. 57, 772, 1967). This effect has been used for Fourier spectrometry (Lohmann, Proc. I.C.O. Conf. on Opt. Instr., London, 1961). We will briefly describe this Fourier spectrometer and then explain how it can be generalized into a spectrometric scanner. By "spectrometric scanner" we mean an instrument which collects information as a function of wavelength λ and of the source coordinates.

Consider figure 2, but for the moment not quite as general as shown. A monochromatic point source may be located on-axis (not off-axis as in figure 2) in the front focal plane of a lens. The resulting plane wave $\exp(i K Z)$ falls onto a grating in plane $Z = 0$. The complex light amplitude immediately behind the grating is

$$U(X, 0) = 1 + \cos(2\pi X/d) = 1 + 1/2\ e^{+iK\lambda X/d} + 1/2\ e^{-iK\lambda X/d}. \quad (9.1)$$

Herein K is as usual $K = 2\pi/\lambda$. The second form of $U(X, 0)$ is meaningful because each term causes a plane wave in the half-space $Z \geq 0$ behind the grating

$$U(X, Z) = e^{iKZ} + 1/2\ e^{iK(X\lambda/d + Z\sqrt{1-(\lambda/d)^2})} + 1/2\ e^{iK(-X\lambda/d + Z\sqrt{1-(\lambda/d)^2})}. \quad (9.2)$$

The validity of this plane wave representation of the wavefield $U(X, Z)$ can be

checked easily by inserting it into the wave equation $(\nabla^2 + K^2)U = 0$. We re-write $U(X, Z)$ into a form which is convenient for computing the intensity $I(X, Z; \lambda) = |U(X, Z)|^2$,

$$U(X, Z) = e^{iKZ}\,[1 + \cos(2\pi X/d)\; e^{-iKZ\{1-\sqrt{1-(\lambda/d)^2}\}}];$$

$$I(X, Z; \lambda) = 1 + \cos^2(2\pi X/d) + 2\cos(2\pi X/d)\cos[KZ\{1 - \sqrt{\ldots}\}]$$

$$= 3/2 + 1/2\cos(4\pi X/d) + 2\cos(2\pi X/d)\cos[KZ\{1 - \sqrt{\ldots}\}];$$

$$\cos[KZ\{1 - \sqrt{\ldots}\}] \approx \cos(\pi Z\lambda/d^2). \qquad (9.3)$$

The important feature about the intensity distribution $I(X, Z; \lambda)$ is its longitudinal periodicity with a period ΔZ,

$$\Delta Z = \frac{2\pi}{K\{1 - \sqrt{\ldots}\}} = \frac{\lambda}{1 - \sqrt{\ldots}} \approx \frac{2d^2}{\lambda} \qquad (9.4)$$

In other words at distances ΔZ, $2\Delta Z$, $3\Delta Z$ the intensity is the same as in $Z = 0$ immediately behind the grating. Hence it is justified to speak about "self-imaging" of a grating which has been illuminated by a monochromatic plane wave. At certain intermediate planes where the "modulation factor" $\cos(\pi Z\lambda/d^2)$ is minus one the contrast of $I(X, Z; \lambda)$ will be reversed, while at yet other planes the modulation factor will be zero, which means that $I(X, Z; \lambda)$ has no contrast in the fundamental lateral period d.

Now let us consider how this "Talbot effect" can be used for spectrometric purposes. Suppose the light source consists of a doublet, λ and $\lambda + \delta\lambda = \lambda(1 + 1/N)$. The total intensity $I(X, Z; \lambda) + I(X, Z; \lambda + \delta\lambda)$ will consist of two parts with slightly different longitudinal periods $\Delta Z(\lambda) = 2d^2/\lambda$ and $\Delta Z(\lambda + \delta\lambda) = 2d^2/(\lambda + \delta\lambda)$. Both parts coincide closely behind the grating at $Z = 0$, but they will get increasingly out of step at larger distances Z. In particular at $Z_0 = Nd^2/\lambda$ the two parts will cancel each others' modulation since the two modulation factors have opposite signs,

$$\cos(\pi Z_0\lambda/d^2) = \cos(\pi N);$$

$$\cos\{\pi Z_0(\lambda + \delta\lambda)/d^2\} = \cos\{\pi(N + 1)\}. \qquad (9.5)$$

Hence the doublet separation $\delta\lambda = \lambda/N$ can be deduced from the distance Z_0 at which zero-modulation is observed: $\delta\lambda = d^2/Z_0$.

For a source with a more general spectral distribution $S(\lambda)$ the total intensity will be

$$\int S(\lambda)\; I(X, Z; \lambda)\; d\lambda = I(X, Z). \qquad (9.6)$$

Measuring the lateral modulation of $I(X, Z)$ for various distances Z yields essentially the same information as a Fourier spectrometer:

$$\int S(\lambda)\cos(\pi Z\lambda/d^2)\; d\lambda. \qquad (9.7)$$

The only difference is that the Fourier transform is carried out as a function of λ and not $1/\lambda$ as usual. The actual measurement of the modulation of $I(X, Z)$ is done by placing a second grating at a distance Z behind the first grating (see figure 2). The second grating, which has the same grating constant d is moved laterally with velocity v_x and the transmitted intensity is collected and measured by a receiver RCV. The amplitude of the a.c. part of the photoelectric signal with the time-frequency v_x/d represents the modulation term

$$\int S(\lambda) \cos(\pi Z\lambda/d^2)\, d\lambda.$$

Now let us consider how such an instrument can gather information also about the geometrical structure of the source $S(\alpha, \beta, \lambda)$. For simplicity let us assume for the moment a monochromatic point source but no longer on-axis. If the point source is shifted vertically no change occurs in the intensity distribution $I(X, Z; \lambda)$ behind the first grating. (This statement is correct only if $Z\lambda^3/d^4 << 1$.) But if the point source is shifted laterally by an amount f tan α the intensity distribution will be "skewed" to $I(X + Z \tan \alpha, Z; \lambda)$. Hence the horizontal shift would show up as a phase delay in the temporal a.c. signal.

In this form our instrument would "see" only the horizontal but not the vertical structure of the source. In order to overcome this limitation we propose to spin the whole instrument around the Z-axis with an angular velocity ω. At the same time we move the second grating laterally with velocity v_x and also longitudinally with velocity v_Z because we want to measure the x-modulation at all distances Z. It is plausible that three types of movements are needed because we convert the three-dimensional source information $S(\alpha, \beta, \lambda)$ into a one-dimensional time signal, the photoelectrical current. Each movement introduces a temporal carrier frequency in the photoelectrical signal. We started to investigate how the choice of the movement parameters ω, v_x, v_Z will ultimately influence the resolution in three dimensions of $S(\alpha, \beta, \lambda)$. The proper choice of these parameters is also important in order to make sure that the three-dimensional object $S(\alpha, \beta, \lambda)$ can be deduced unambiguously from the one-dimensional photoelectrical current.

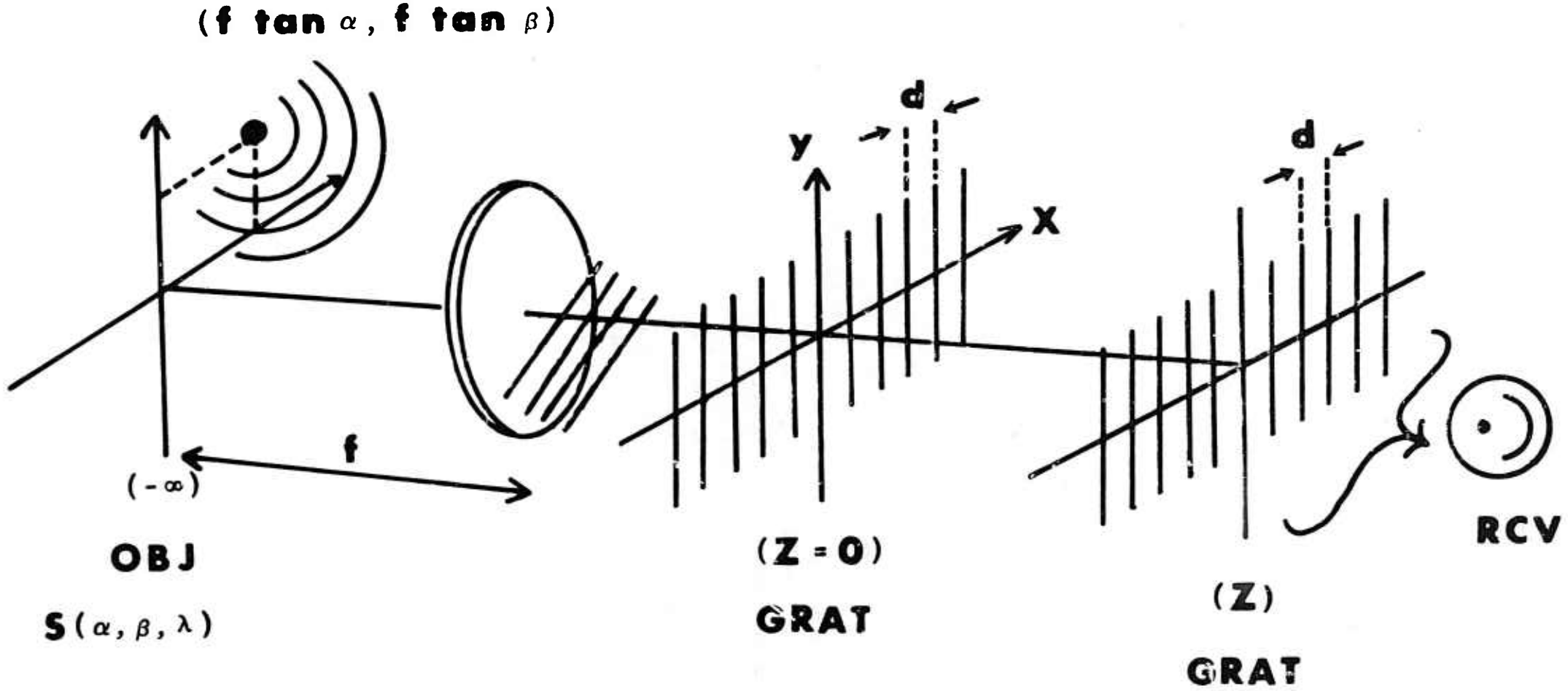

Figure 2
Basic Setup of the Multiplex Scanner

§10 Signal Flow from Sky to Tape

The object signal is the radiation $S(\alpha, \beta, \sigma)$ coming from the sky. S might also vary as a function of time. But we assume these temporal variations to be slow compared to the azimuthal scanning cycle of the instrument. The m-th color filter $F_m(\sigma)$ selects the spectral component S_m

$$S_m(\alpha, \beta) = \int S(\alpha, \beta, \sigma)\, F_m(\sigma)\, d\sigma. \tag{10.1}$$

The j-th neutral density filter reduces the signal by a factor T_j;

$$T_j\, S_m(\alpha, \beta) = S_{mj}(\alpha, \beta). \tag{10.2}$$

The chopper acts multiplicatively like

$$S_{mj}(\alpha, \beta) \sum A_\ell\, e^{2\pi i \ell \nu_c t}. \tag{10.3}$$

Only the fundamental chopper frequency ($|\ell| = 1$) will later pass through the electronic amplifier. Hence it is enough to consider the $|\ell| = 1$ term as the signal which enters the optical system of the telescope,

$$S_{mj}(\alpha, \beta)\ 2\ A_1 \cos(2\pi\nu_c t). \tag{10.4}$$

Now we must relate the sky coordinates α, β to the coordinates x', y' in the image plane of the telescope. An auxilliary coordinate system x, y, z is defined with its origin in the center of the telescope's lens (see figures 3, 4 and 5). The z-axis is also the gondola's axis pointing towards the zenith $\beta = 0$. The x-axis points to the magnetic north pole at azimuth angle $\alpha = 0$, and the y-axis is perpendicular to both x- and z-axes. Presently the telescope axis may be pointed towards α_1, β_1. Hence the sky coordinates α_1, β_1 are projected into the center $x' = 0$, $y' = 0$ of the telescope's image plane. A sky point close to α_1, β_1 in $\alpha = \alpha_1 + \alpha'$, $\beta = \beta_1 + \beta'$ will occur at $x' = \alpha' f \sin\beta_1$, $y' = \beta' f$ in the image plane. The letter f stands for focal length. We have used the small angle approximation $\tan\alpha' \approx \alpha'$, $\tan\beta' \approx \beta'$, which is justified since the receivers in the image plane are all very close to $x' = 0$, $y' = 0$. The factor $\sin\beta_1$ in $x' = \alpha' f \sin\beta_1$ describes the fact that two meridians separated by α' are getting closer together near the zenith $\beta = 0$ (see figure 5).

The quality of the telescope's lens system is described by its point spread function M or by its transfer function $\tilde{M}$:

$$M(x', y') = \iint \tilde{M}(\nu, \mu)\, e^{2\pi i (x'\nu + y'\mu)}\, d\nu d\mu. \tag{10.5}$$

Hence a point on the sky at $\alpha_1 + \alpha'$, $\beta_1 + \beta'$ will produce as radiation distribution in the image plane the point spread function centered at $x' = \alpha' f \sin\beta_1$, $y' = \beta' f$. In mathematical symbols,

$$\delta(\alpha - \alpha_1 - \alpha', \beta - \beta_1 - \beta') \rightarrow M(x' - \alpha' f \sin\beta_1, y' - \beta' f). \tag{10.6}$$

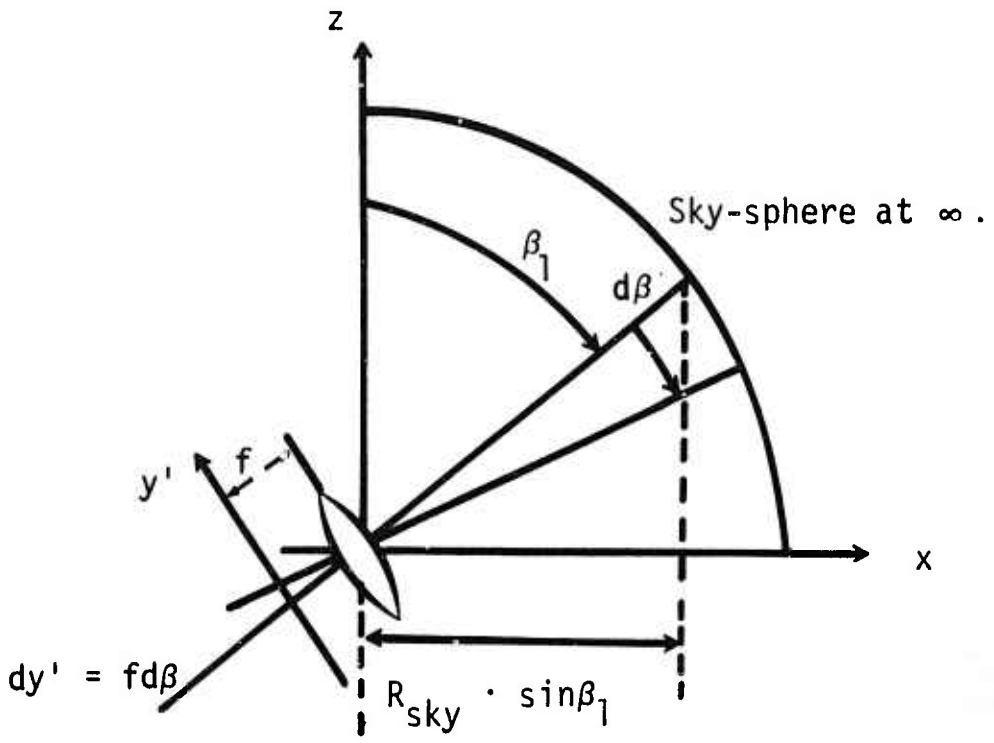

Figure 3

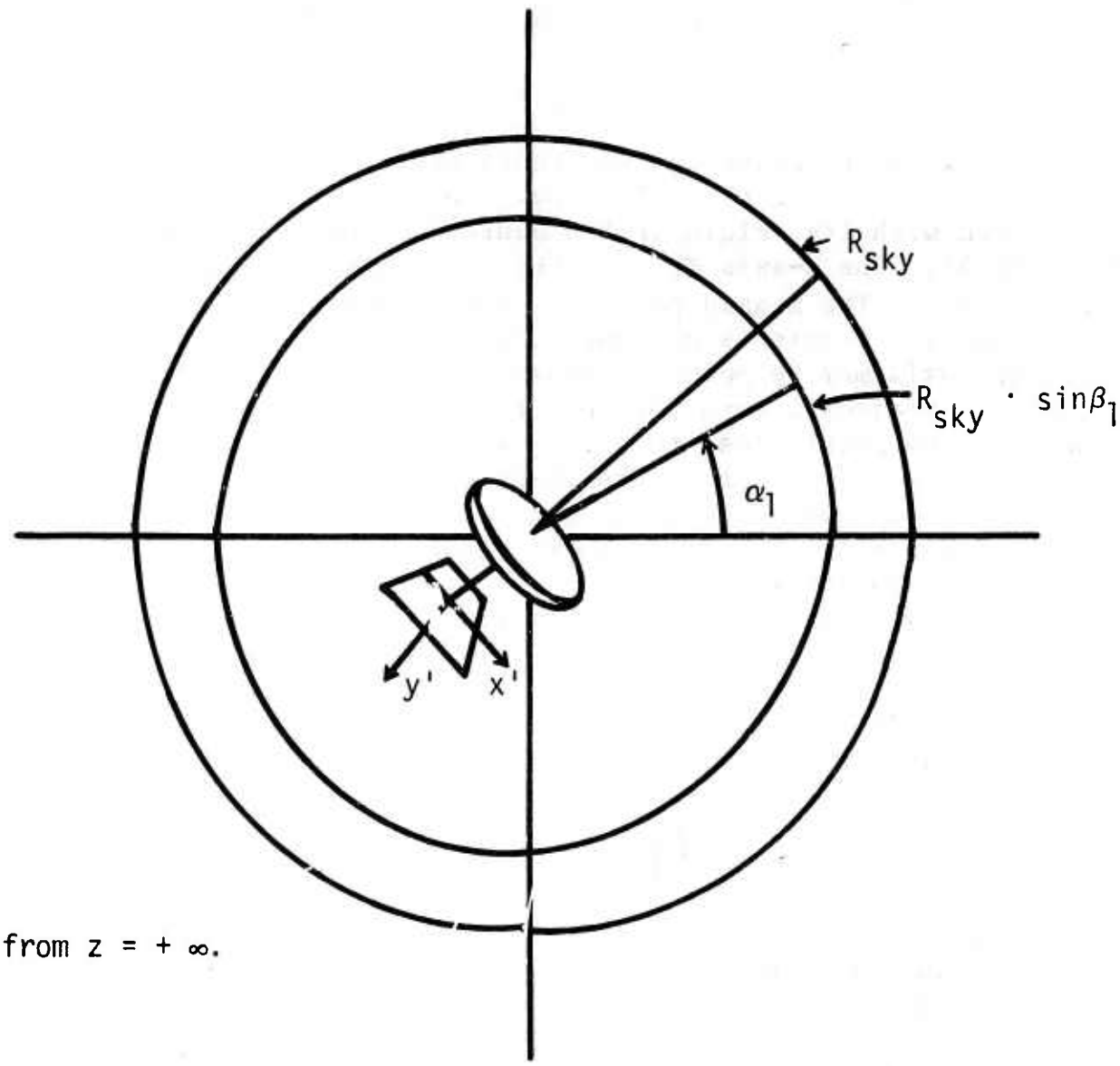

View from z = + ∞.

Figure 4

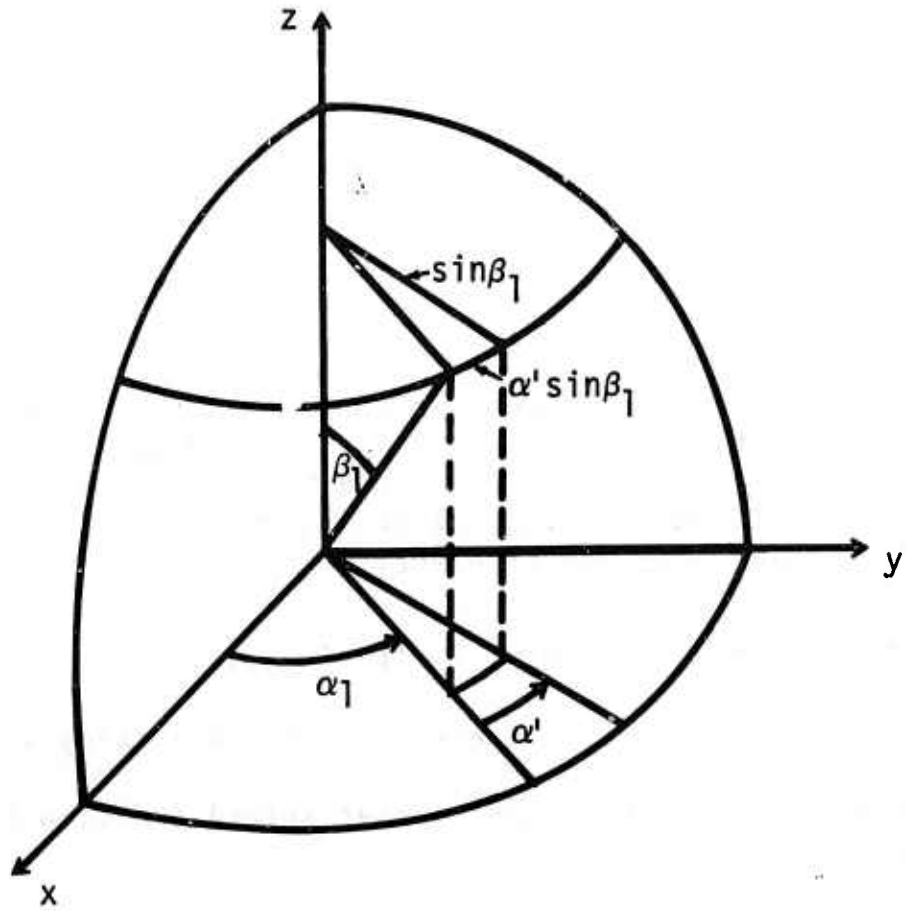

Figure 5

If the point source gets stronger by a factor of say $S_{mj}(\alpha_1 + \alpha', \beta_1 + \beta')$ then also the radiation in the image plane gets stronger by the same factor:

$$S_{mj}(\alpha_1 + \alpha', \beta_1 + \beta')\ \delta(\alpha - \alpha_1 - \alpha', \beta - \beta_1 - \beta')$$

$$\rightarrow S_{mj}(\alpha_1 + \alpha', \beta_1 + \beta')\ M(x' - \alpha' f \sin\beta_1, y' - \beta' f). \qquad (10.7)$$

All these point sources together form the signal on the sky, whereby the spectral and density filters F_m and f_j are already taken into account:

$$\iint S_{mj}(\alpha_1 + \alpha', \beta_1 + \beta')\ \delta(\alpha - \alpha_1 - \alpha', \beta - \beta_1 - \beta')\ d\alpha' d\beta'$$

$$= S_{mj}(\alpha, \beta). \qquad (10.8)$$

Because the telescope system is linear in radiative power the effect of $S_{mj}(\alpha, \beta)$ in the image plane is computed by the convolution of S_{mj} and M:

$$\iint S_{mj}(\alpha_1 + \alpha', \beta_1 + \beta')\ M(x' - \alpha' f \sin\beta_1, y' - \beta' f)\ d\alpha' d\beta'. \qquad (10.9)$$

Only what falls onto the receiver can contribute to the photoelectronic signal. This can be described in mathematical terms by multiplying the above expression by the receiver weighting function R(x', y') and then integrating it over x', y'. The R is "1" where the receiver is, and "0" elsewhere. For the time being let us consider only one receiver:

$$\iiiint S_{mj}(\alpha_1 + \alpha', \ldots)\ M(x' - \alpha' f \sin\beta_1, \ldots)$$

$$R(x', y')\ d\alpha'\ d\beta'\ dx' dy'. \qquad (10.10)$$

The terms M and R together describe the angular spread function P of the scanning telescope:

$$\iint S_{mj}(\alpha_1 + \alpha', \beta_1 + \beta')\ P(-\alpha' \sin\beta_1, -\beta')\ d\alpha' d\beta';$$

$$P(-\alpha' \sin\beta_1, -\beta') = \iint M(x' - \alpha' f \sin\beta_1, y' - \beta' f)\ R(x', y')\ dx' dy'$$

$$= \iint \tilde{M}(-\nu, -\mu)\ \tilde{R}(\nu, \mu)\ e^{2\pi i(\nu\alpha' f \sin\beta_1 + \mu\beta' f)}\ d\nu d\mu. \qquad (10.11)$$

Due to the torsion oscillation the azimuth angle α_1 of the telescope axis varies according to

$$\alpha_1 = \alpha_M \sin\{2\pi\Omega(t - t_0)\}. \qquad (10.12)$$

During time intervals long compared to the chopper period $1/\nu_c$ we can approximate

$$\alpha_1 \approx \omega(t - t_0). \qquad (10.13)$$

But ω will be different in different time intervals. It can be computed

as the derivative of $\alpha_1(t)$,

$$\omega = \omega(t) = d\alpha_1/dt = 2\pi\Omega\ \alpha_M \cos\{2\pi\Omega(t - t_0)\ . \qquad (10.14)$$

Now we have followed the signal from the sky into the receiver where it is

$$2\ A_1 \cos(2\pi\nu_c t) \iint S_{mj}(\omega\{t - t_0\} + \alpha',\ \beta_1 + \beta')$$
$$P(-\alpha' \sin\beta_1,\ -\beta')\ d\alpha' d\beta' = U_{mj}(t). \qquad (10.15)$$

The next step is the addition of receiver noise n(t), which is supposed to be independent of the signal, and specified only by its power spectrum $|\tilde{n}(\nu_t)|^2$. Signal and noise together are subjected to an electrical filter with transfer function $\tilde{G}(\nu_t)$ before being recorded on tape as $U_R(t)$:

$$U_R(t) = [U_{mj}(t) + n(t)]^* G(t) =$$
$$= \int [\tilde{U}_{mj}(\nu_t) + \tilde{n}(\nu_t)]\ \tilde{G}(\nu_t)\ e^{2\pi i \nu_t t}\ d\nu_t. \qquad (10.16)$$

§11 Influence of the Neutral Density Filters T_j

The neutral density filters may have transmittance factors of $T_0 = 1$, $T_1 = 10^{-1}$, $T_2 = 10^{-2}$, for example. The recorded signal will suddenly change by a factor of 10 whenever the servo demands a filter change. These jumps are disquieting at first sight for two reasons: the jumps need a finite amount of time during which we loose the genuine signal; we don't know how to define the average signal power spectrum, which is an important quantity for the digital signal restoration process (see §5).

To answer the latter question first the reason for switching the neutral density filters T_j at proper occasions is of course to maintain a suitable power level arriving at the receiver. In other words the signal power spectrum at the receiver is essentially always the same, no matter which neutral density filter T_j happens to be in operation. The short times it takes to exchange the T_j filters must be excluded when computing the average signal power spectrum because this transition has nothing to do with the genuine signal.

During the short filter exchange times the signal is lost. But this is not severe because there are actually four receivers in the image plane of the telescope. A given point on the sky is observed at slightly different times by the four receivers. The T_j - filter may or may not be switched simultaneously for the four receivers depending on whether the pivot point of the filter wheel is in-line with the four receivers or far off the line of receivers (see figure 6). Even more generality would be achieved if the edges of the filter sections were not straight lines coming from the pivot point.

In any event when plotting in an α,t-diagram the dead times and the

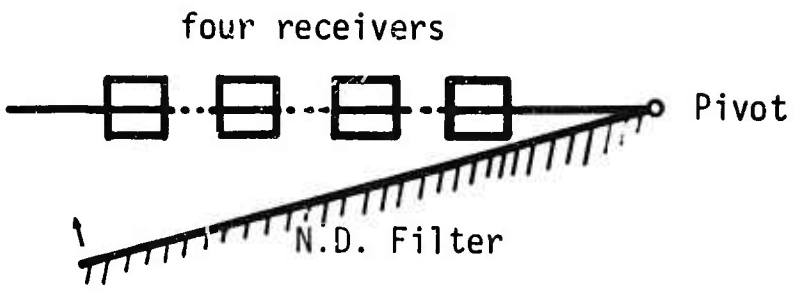

Simultaneously

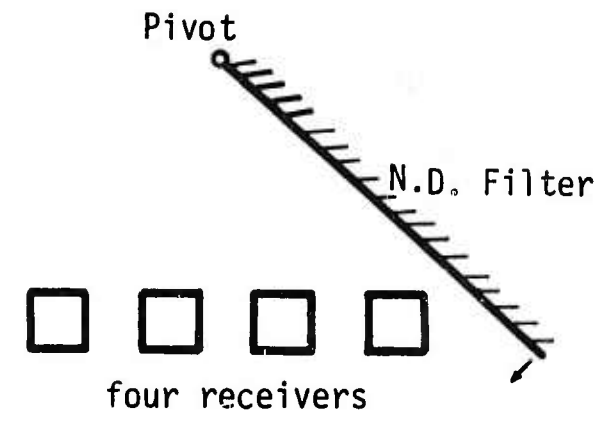

Sequentially from the right

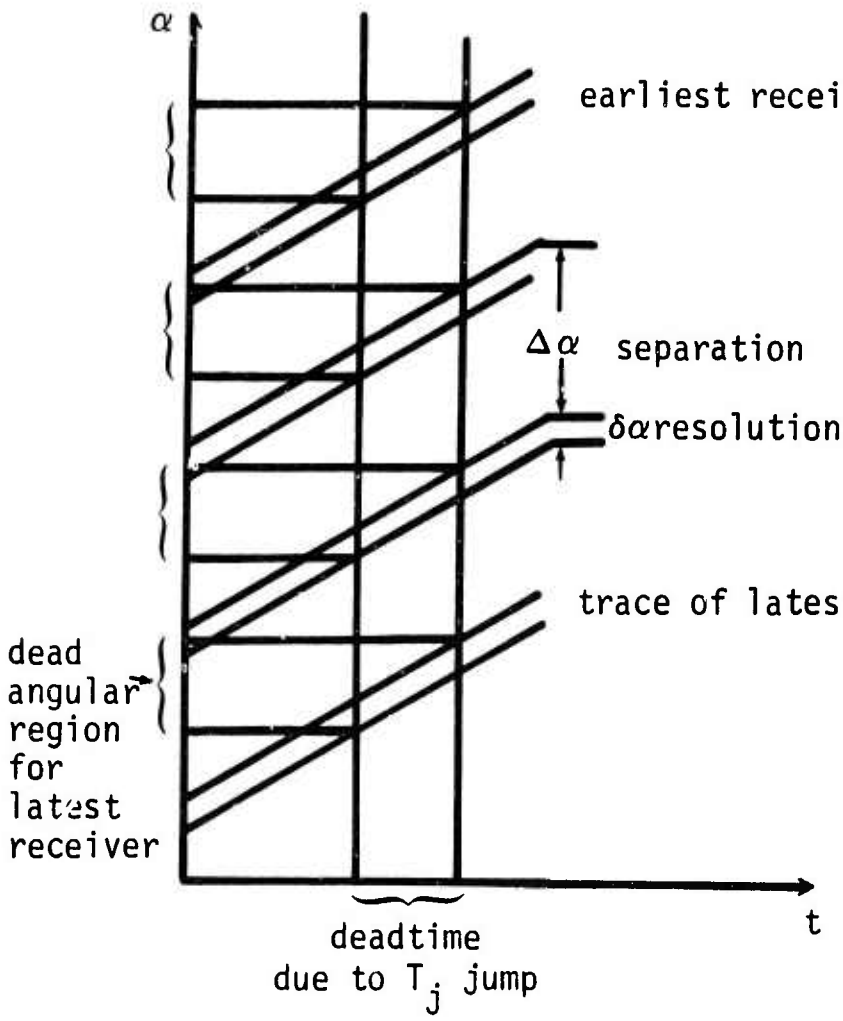

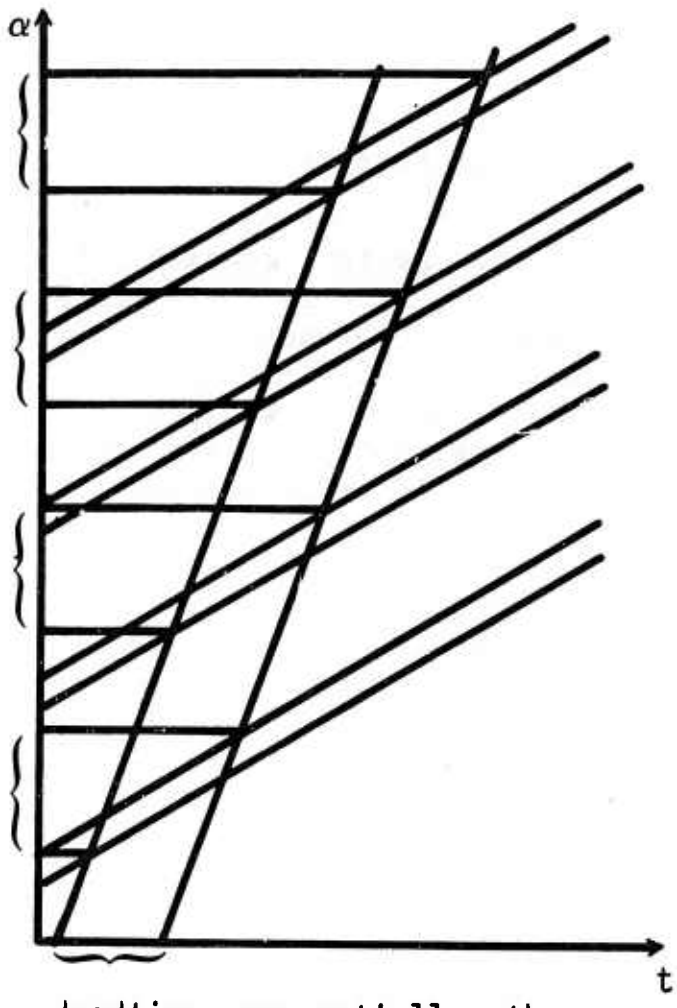

Figure 6

resulting dead angles for the four receivers (figure 6) it becomes apparent that it is preferable to let the dead times for the four receivers occur sequentially. The latest receiver should be switched first. "Latest" means that this receiver scans a certain sky point always later than the other three receivers. However, the property of "latest" is converted to "earliest" after the torsion oscillation has reached the reversal angle $\alpha = \pm \alpha_M$. Furthermore the filter wheel has to be turned sometimes from T_j to T_{j+1}, but also sometimes in reverse from T_{j+1} to T_j. Hence as a compromise it is sensible to apply simultaneous switching. The switching dead time should be shorter than the time it takes to scan from α to $\alpha + \Delta\alpha$, where $\Delta\alpha$ is the angular separation of two adjacent receivers.

§12 Dilute β-Scanning

The available observation time is not very long, allowing only a small number of α-revolutions, maybe 10 or 20. Hence the elevation steps $\Delta\beta$ must be relatively coarse, say 5°. This is much more than the diameter $\delta\beta$ of the angular spread function P of the telescope (lens and receiver considered). This has two consequences: we don't know anything about object points midway between two β-scans, say at β_1 and at $\beta_2 = \beta_1 + \Delta\beta$. Furthermore our measurements are somewhat ambiguous. This can be understood with the help of figure 7, where parts of $\int P(\alpha', \beta - \beta_1)\, d\alpha'$ and $\int P(\alpha', \beta - \beta_2)\, d\alpha'$ are plotted. These plots are in effect weighting functions indicating if and how strong a sky point α, β will occur in the recorded signal. The ambiguity becomes obvious when considering two object points at α_0, β_1 and at α_0, $\beta_1 + \varepsilon$, the first point being weaker than the second one. Nevertheless the recorded signals could be indistinguishable. Even a line object of the form $\delta(\alpha - \alpha_0)$ would produce the same type of a recorded signal. L. Biberman in his book on "Reticles in Electro-Optical Devices" (Pergamon 1966) also discusses this ambiguity in length. He concurs that this ambiguity cannot be removed, except by decreasing the scanning step $\Delta\beta$ or by providing some additional information about the object (see §14).

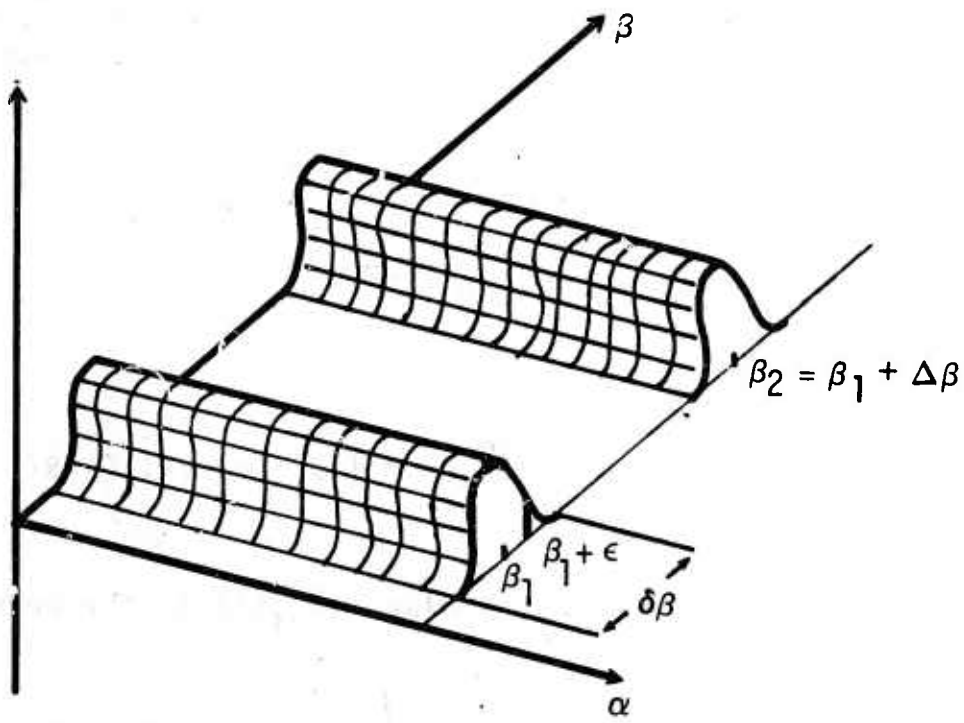

Figure 7

Since these openings don't exist in general we have to admit the ambiguity and try to make the best of it. This implies that we might replace the unknown signal $S_{mj}(\alpha_1 + \alpha', \beta_1 + \beta')$ by an equivalent signal $S_E(\alpha_1 + \alpha', \beta_1 + \beta')$ which appears to be the same to our scanning telescope:

$$\iint S_{mj}\, P(-\alpha' \sin\beta_1, -\beta')\, d\alpha' d\beta' = \iint S_E\, P(-\alpha' \sin\beta_1, -\beta')\, d\alpha' d\beta'. \tag{12.1}$$

There exists an infinite variety of S_E models, from which we may choose the one which is most convenient in terms of mathematical manipulations and experimental test procedures. Two of the most obvious choices are

$$S_{mj}(\alpha, \beta_1 + \beta') = S_D(\alpha)\ \delta(\beta')$$

$$S_{mj}(\alpha, \beta_1 + \beta') = S_E(\alpha)\ \mathrm{rect}\ (\beta'/\delta\beta). \tag{12.2}$$

The second model turns out to be very convenient. Herein the rect-function is "one" within $-\delta\beta/2 \le \beta' \le \delta\beta/2$ and "zero" elsewhere. For the second model we get

$$\iint S_{mj}\, P\, d\alpha' d\beta' = \iint S_E(\alpha_1 + \alpha')\ \mathrm{rect}(\beta'/\delta\beta)\ \ P(-\alpha' \sin\beta_1, -\beta')\, d\alpha' d\beta'$$

$$= \int S_E(\alpha_1 + \alpha') \left[\int \mathrm{rect}(\beta'/\delta\beta)\ P(-\alpha' \sin\beta_1, -\beta')\, d\beta' \right] d\alpha'. \tag{12.3}$$

In the square bracket we can disregard the rect-function because P itself is anyway zero outside of $|\beta'| \le \delta\beta/2$. The square-bracket is therefore the angular line-spread function L:

$$\int P(-\alpha' \sin\beta_1, -\beta')\, d\beta' = L(-\alpha' \sin\beta_1). \tag{12.4}$$

The line-spread function is easier to measure than the point-spread function because test objectsmay be infinitely extended in the β-direction. L can be deduced from the lens transfer function $\tilde{M}$ and from the spatial spectrum $\tilde{R}$ of the receiver,

$$L(-\alpha' \sin\beta_1) = \iiint \tilde{M}(-\nu, -\mu)\ \tilde{R}(\nu, \mu)\ e^{2\pi i(\nu\alpha' f \sin\beta_1 + \mu\beta' f)}\, d\nu d\mu d\beta'$$

$$= \frac{1}{f} \int \tilde{M}(-\nu, 0)\ \tilde{R}(\nu, 0)\ e^{2\pi i \nu\alpha' f \sin\beta_1} d\nu;$$

$$\tilde{L}(\nu) = \int L(\alpha)\ e^{-2\pi i \nu\alpha}\, d\alpha = (f)^{-2}\ \tilde{M}(\nu/f, 0)\ \tilde{R}(-\nu/f, 0). \tag{12.5}$$

With the equivalent object S_E the signal $U_{mj}(t)$ in the receiver (see §2) is:

$$U_{mj}(t) = 2\ A_1 \cos(2\pi\nu_c t) \int S_E(\omega\{t - t_0\} + \alpha')\ L(-\alpha' \sin\beta_1)\, d\alpha'. \tag{12.6}$$

Roughly speaking U_{mj} resulted from S_E after it had been filtered by $\tilde{L}$ and modulated with chopper frequency ν_c. The next steps (12.7) are addition of noise n(t), and filtering in the electronic system by $\tilde{G}(\nu_t)$, and recording on tape as $U_R(t)$. These steps are best described in the temporal frequency domain:

$$\tilde{U}_R(\nu_t) = \{\tilde{U}_{mj}(\nu_t) + \tilde{n}(\nu_t)\}\ \tilde{G}(\nu_t);$$

$$\tilde{U}_{mj}(\nu_t) = \int U_{mj}(t)\ e^{-2\pi i\nu_t t}\ dt =$$

$$= A_1 \iint e^{+2\pi i\nu_c t}\ S_E\ L\ e^{-2\pi i\nu_t t}\ d\alpha' dt +$$

$$+ A_1 \iint e^{-2\pi i\nu_c t}\ S_E\ L\ e^{-2\pi i\nu_t t}\ d\alpha' dt =$$

$$= \frac{A_1}{\omega\ \sin\beta_1}\ e^{-2\pi i\nu_t t_0}\left[\tilde{S}_E\left(\frac{\nu_t - \nu_c}{\omega}\right)\tilde{L}\left(\frac{\nu_t - \nu_c}{\omega\ \sin\beta_1}\right)e^{+2\pi i\nu_c t_0} +\right.$$

$$\left. + \tilde{S}_E\left(\frac{\nu_t + \nu_c}{\omega}\right)\tilde{L}\left(\frac{\nu_t + \nu_c}{\omega\ \sin\beta_1}\right)e^{-2\pi i\nu_c t_0}\right]. \qquad (12.7)$$

§13 Signal Restoration by Digital Filtering

After having recorded $U_R = [U_{mj} + n]*G$ we want to recover from it as well as possible the original signal $S_E(\alpha)$. The term "as well as possible" is meant in the root-mean square sense. The recovery procedure will consist of a linear filtering process which may be performed digitally. Before actually determining which filter function $\tilde{D}$ is optimal we will recall briefly the classical Wiener-filter problem and generalize it somewhat.

Suppose an object signal U(x) has been corrupted by additive noise n(x). What is the best convolution function H(x) for object restoration?

$$\int H(x - x')\ \{U(x') + n(x')\}\ dx' \overset{?}{\approx} U(x). \qquad (13.1)$$

Wiener found an H(x) which achieves the job optimal in the least-mean-square sense. For computing H(x) or its Fourier transform the so-called Wiener-filter $\tilde{H}(\nu)$ we must know the power spectra $|\tilde{U}(\nu)|^2$ and $|\tilde{n}(\nu)|^2$ of object and noise,

$$\int \left| U(x) - \int H(x - x') \{U(x') + n(x')\} dx' \right|^2 dx \to \text{MINIMUM};$$

$$\tilde{H}(\nu) = \frac{|\tilde{U}(\nu)|^2}{|\tilde{U}(\nu)|^2 + |\tilde{n}(\nu)|^2}; \qquad H(x) = \int \tilde{H}(\nu)\, e^{2\pi i \nu x}\, d\nu. \tag{13.2}$$

The minimum requirement above can be translated into an equivalent minimum requirement in the Fourier domain,

$$\int |\tilde{U}(\nu) - \tilde{H}(\nu) \{\tilde{U}(\nu) + \tilde{n}(\nu)|^2 \, d\nu \to \text{MINIMUM}. \tag{13.3}$$

For this "Fourier translation" we made use of the Plancherel theorem and of the convolution theorem

$$\int |f(x)|^2 dx = \int |\tilde{f}(\nu)|^2 d\nu;$$

$$\int H(x - x')\, V(x')\, dx' = \int \tilde{H}(\nu)\, \tilde{V}(\nu)\, e^{2\pi i \nu x}\, d\nu. \tag{13.4}$$

The Fourier version of the minimum requirement is very convenient for a generalization which we study now.

Let us assume that u is filtered by $\tilde{L}$ *before* noise is added:

$$\tilde{u}(\nu) \to \tilde{u}(\nu)\, \tilde{L}(\nu) \to \tilde{u}(\nu)\, \tilde{L}(\nu) + \tilde{n}(\nu). \tag{13.5}$$

Now the modulus of the minimization integral is

$$|\tilde{u}(\nu) - \tilde{H}_1(\nu)\{\tilde{u}(\nu)\, \tilde{L}(\nu) + \tilde{n}(\nu)\}| = |\tilde{u}(\nu) - \tilde{H}_1(\nu)\, \tilde{L}(\nu)\{\tilde{u}(\nu) + \tilde{n}(\nu)/\tilde{L}(\nu)\}|. \tag{13.6}$$

Hence the Wiener-type derivation, which led to $\tilde{H}(\nu)$, can be performed as before, except that $\tilde{n} \to \tilde{n}/\tilde{L}$ and $\tilde{H} \to \tilde{H}_1\tilde{L}$.

$$\tilde{H}_1\tilde{L} = \frac{|\tilde{u}|^2}{|\tilde{u}|^2 + |\tilde{n}/} \; ; \qquad \tilde{H}_1(\nu) = \frac{|\tilde{L}(\nu)\, \tilde{u}(\nu)|^2}{\tilde{L}(\nu)\{|\tilde{L}\tilde{u}|^2 + |\tilde{n}|^2\}}. \tag{13.7}$$

Now let us be one more step [illegible] additional filter process $\tilde{G}(\nu)$ may be part of the system *after* the [illegible]n:

$$\tilde{u} \to \tilde{u}\tilde{L} \to \tilde{u}\tilde{L} + \tilde{n} \to \tilde{u}\tilde{L}\tilde{G} + \tilde{n}\tilde{G}. \tag{13.8}$$

We look now for a filter $\tilde{H}_2$, which minimizes

$$\int |\tilde{u}(\nu) - \tilde{H}_2(\nu)\, \tilde{G}(\nu)\{\tilde{u}(\nu)\, \tilde{L}(\nu) + \tilde{n}(\nu)\}|^2 \, d\nu = \int |\tilde{u} - \tilde{H}_2\tilde{G}\, \tilde{L}\{\tilde{u} - \tilde{n}/\tilde{L}\}|^2 \, d\nu. \tag{13.9}$$

This has again the "Wiener shape", but with $\tilde{n}/\tilde{L}$ instead of $\tilde{n}$, and with $\tilde{H}_2\tilde{G}\tilde{L}$

instead of $\tilde{H}$,

$$\tilde{H}_2\tilde{G}\,\tilde{L} = \frac{|\tilde{u}|^2}{|\tilde{u}|^2 + |\tilde{n}/\tilde{L}|^2} = \frac{|\tilde{u}\tilde{L}|^2}{|\tilde{u}\tilde{L}|^2 + |\tilde{n}|^2}$$

$$\tilde{H}_2(\nu) = \frac{1}{\tilde{G}(\nu)\,\tilde{L}(\nu)} \cdot \frac{|\tilde{u}(\nu)\,\tilde{L}(\nu)|^2}{|\tilde{u}(\nu)\,\tilde{L}(\nu)|^2 + |\tilde{n}(\nu)|^2} \qquad (13.10)$$

(inverse filter) (Wiener weighting function)

The last Wiener-generalization has already almost the form we need as can be seen at the end of §12. The corresponding terms are: $\tilde{S}_E \sim \tilde{U}$; $\tilde{L} \sim \tilde{L}$; $\tilde{G} \sim \tilde{G}$. However the signal term $\tilde{S}_E$ occurs with a frequency shift of $\pm\,\nu_c$ due to the chopper modulation. Hence we first must demodulate our tape recorded signal. We do this by first multiplying it with $2\cos\{2\pi\,\nu_c(t - t_0)$ and then rejecting by means of a low-pass filter all terms which still contain ν_c in some form.

For a general function $f(t) = \int \tilde{f}(\nu)\, e^{2\pi i\nu t}\, d\nu$ the process of multiplying it $\cdot\, 2\cos\{2\pi\,\nu_c(t - t_0)$ means

$$\tilde{f}(\nu) \to \tilde{f}(\nu - \nu_c)\, e^{-2\pi i t_0 \nu_c} + \tilde{f}(\nu + \nu_c)\, e^{+2\pi i t_0 \nu_c}. \qquad (13.11)$$

For the specific function of interest the recorded signal $\{U_{mj} + n\}*G = U_R$ means

$$\tilde{U}_R(\nu_t) = \{\tilde{U}_{mj}(\nu_t) + \tilde{n}(\nu_t)\,\tilde{G}(\nu_t) \to$$

$$\tilde{U}_{mj}(\nu_t - \nu_c)\,\tilde{G}(\nu_t - \nu_c)\, e^{-2\pi i t_0 \nu_c} + \tilde{U}_{mj}(\nu_t + \nu_c)\,\tilde{G}(\nu_t + \nu_c)\, e^{+2\pi i t_0 \nu_c} +$$

$$+ \tilde{n}(\nu_t - \nu_c)\,\tilde{G}(\nu_t - \nu_c)\, e^{-2\pi i t_0 \nu_c} + \tilde{n}(\nu_t + \nu_c)\,\tilde{G}(\nu_t + \nu_c)\, e^{+2\pi i t_0 \nu_c}. \qquad (13.12)$$

We insert the expression for $\tilde{U}_{mj}(\nu_t)$ from §12 and neglect all terms with $\pm\,2\,\nu_c$ which will be rejected by the lowpass filter

$$\tilde{U}_{mj}(\nu_t) = \frac{A_1\, e^{-2\pi i \nu_t t_0}}{\omega\,\sin\beta_1}\,[\ldots];$$

$$[\ldots] = \tilde{S}_E\left(\frac{\nu_t - \nu_c}{\omega}\right)\tilde{L}\left(\frac{\nu_t - \nu_c}{\omega\,\sin\beta_1}\right) e^{+2\pi i \nu_c t_0} + (\text{same, but } \nu_c \to -\nu_c). \qquad (13.13)$$

The spectrum of the recorded signal after digital demodulation contains as contribution from the object

$$\tilde{S}_E\left(\frac{\nu_t}{\omega}\right)\tilde{L}\left(\frac{\nu_t}{\omega\,\sin\beta_1}\right)\frac{A_1}{\omega\,\sin\beta_1}\, e^{-2\pi i \nu_t t_0}\,[\tilde{G}(\nu_t - \nu_c)\, e^{-2\pi i \nu_c t_0} +$$

$$\tilde{G}(\nu_t + \nu_c)\, e^{+2\pi i \nu_c t_0}\,; \qquad (13.14)$$

or abbreviated, $\tilde{S}_E\left(\frac{\nu_t}{\omega}\right)\tilde{E}(\nu_t)$. The noise spectrum of the recorded signal will also be renamed for brevity

$$\tilde{n}_E(\nu_t) = \tilde{n}(\nu_t - \nu_c)\,\tilde{G}(\nu_t - \nu_c)\, e^{-2\pi i t_0 \nu_c} + \tilde{n}(\nu_t + \nu_c)$$

$$\tilde{G}(\nu_t + \nu_c)\, e^{+2\pi i t_0 \nu_c}. \qquad (13.15)$$

It is important that the effective noise power spectrum $|\tilde{n}_E(\nu_t)|^2$ can be computed from the original noise power spectrum $|n(\nu_t)|^2$ and from other known properties such as the electrical filter function $\tilde{G}(\nu_t)$:

$$|\tilde{n}_E(\nu_t)|^2 = |\tilde{n}(\nu_t - \nu_c)|^2\ |\tilde{G}(\nu_t - \nu_c)|^2 + |\tilde{n}(\nu_t + \nu_c)|^2\ |\tilde{G}(\nu_t + \nu_c)|^2$$
$$+ \tilde{n}(\nu_t - \nu_c)\ \tilde{n}^*(\nu_t + \nu_c)\ \tilde{G}^*(\nu_t + \nu_c)\ e^{-4\pi i t_0 \nu_c} + \text{conj. compl.} \qquad (13.16)$$

Obviously the first two terms are known. The last two terms can be considered to be zero, at least whenever a ν_t-integration takes place. The phases of $\tilde{n}(\nu_t - \nu_c)$ and of $\tilde{n}^*(\nu_t + \nu_c)$ can be assumed to fluctuate so wildly that any integral will cancel, or at least fluctuate itself so rapidly that the demodulation lowpass filter for $|\nu_t| < \nu_c/2$ will block any contribution.

At this point we found the temporal frequency spectrum of the recorded signal after demodulation was

$$\tilde{U}_D(\nu_t) = \tilde{S}_E\left(\frac{\nu_t}{\omega}\right) \tilde{E}(\nu_t) + \tilde{n}_E(\nu_t). \qquad (13.17)$$

Herein $\tilde{E}$ and $|\tilde{n}_E|^2$ are known and $\tilde{S}_E$ or its Fourier transform $S_E(\alpha)$ is wanted as accurately as possible. The modified Wiener filter suitable for this job is

$$\tilde{D}(\nu_t) = \frac{1}{\tilde{E}(\nu_t)}\ \frac{|\tilde{S}_E(\nu_t/\omega)|^2}{|\tilde{S}_E(\nu_t/\omega)|^2 + |\tilde{n}_E(\nu_t)|^2}\ . \qquad (13.18)$$

§14 A Method for Closing the Gaps of the Dilute β-Scanning

In §12 we had discussed the dilemma which was caused by the fact that the steps $\Delta\beta$ in elevation had to be considerably larger than the resolution $\delta\beta$ in elevation. The factor $\Delta\beta/\delta\beta$ might be about five. The reason for the dilute β-scanning is lack of observation time. Consequently the "image" will have wide gaps in the β-domain. In general these gaps are unavoidable under the given constraints due to the scanning mode of the instruments. However, there might be special circumstances which allow us to close the gaps.

Let us assume there are *only point-objects* on the sky. We propose to replace the four independent receivers by a single receiver which might have for example the shape of a V or an N (figure 8). The height of the V (or the N) is $\Delta\beta$. Hence every point on the sky will have at some time the opportunity to send some light into the extended receiver. We will know of course the $\Delta\beta$-interval for every object point since we keep track of the $\Delta\beta$-steps of the scanning procedure. The fine resolution within a given β-interval can be deduced from the fine structure of the recorded signal. For example a point on the sky which is scanned by the lower part of the V receiver will respond with two peaks close together, while another point a little higher up will produce two peaks somewhat farther apart.

The mathematical procedure for getting fine β-resolution out of the raw

signal $S_m(\alpha)$, which has been collected by scanning with the V-receiver over the strip $(\beta_m, \beta_m + \Delta\beta)$ is as follows: Suppose we want to compute $S(\alpha, \beta_m + i\delta\beta)$; $i = 0, 1, \ldots, I - 1$; $I\delta\beta = \Delta\beta$. The shape of the V may be such that the two bars are apart from each other by $(i + 2)\delta\alpha$ at an elevation $i\beta$ above β_m. If there is a point object on the sky at $(\alpha, \beta_m + i\delta\beta)$ then it will create two pulses in the raw signal $S_m(\alpha)$ at $\alpha + (i + 1)\delta\alpha$ and at $\alpha - (i + 1)\delta\alpha$. We test this by multiplying the signals $S_m\{\alpha + (i + 1)\delta\alpha\}$ and $S_m\{\alpha - (i + 1)\delta\alpha\}$. For adjusting the magnitude of this object point we have to draw the root

$$\sqrt{S_m\{\alpha + (i + 1)\delta\alpha\}\, S_m\{\alpha - (i + 1)\delta\alpha\}} = S(\alpha, \beta_m + i\delta\beta);$$

$$i = 0, 1\ldots, I - 1; \; I\delta\beta = \Delta\beta. \qquad (14.1)$$

In order to achieve β-resolution in $\delta\beta$ steps we have to repeat this operation for all possible double pulse separations. Now $S(\alpha, \beta_m + i\delta\beta)$ is ready for the filtering process described in §13.

Possibly this filtering operation might have to be generalized into two dimensions. But such a study is not warranted at present since it is unknown *if* all or most of the objects are points, and *if* there exists any chance to implement a V-receiver. However, if these two "ifs" are confirmed an additional study is desirable for finding what happens if there are occasionally objects which are not points.

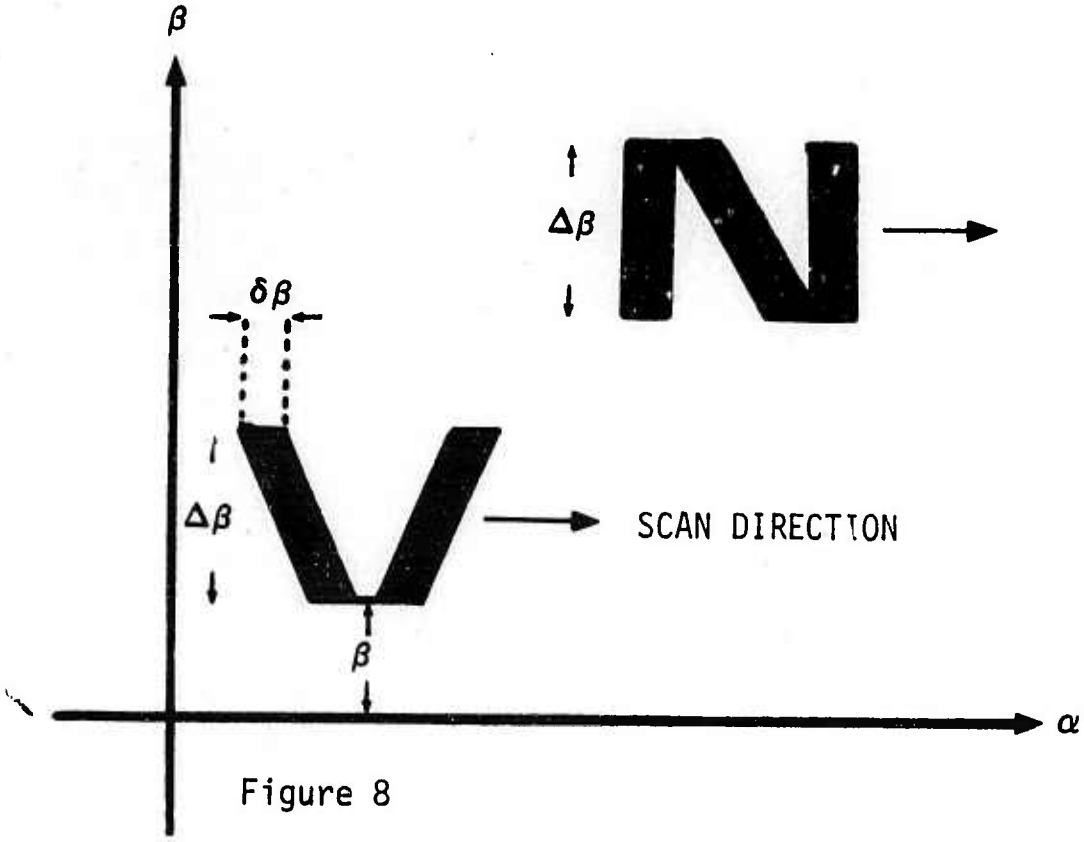

Figure 8

References cited in this report:

"Fourier Images"
Cowley and Moodie, Proc. Phys. Soc. B70, 486, 1957; B76, 378, 1960.

"Self-Imaging"
Montgomery, J. Opt. Soc. Am. 57, 772, 1967.

"A New Fourier Spectrometer"
Lohmann, Proc. ICO Conf. Opt. Inst., London 1961, Butterworth.

List of all participating scientists:

Adolf W. Lohmann, principal investigator, professor of applied physics;

Donald Silva, research assistant.

Statement about related contracts and publications:

This is the first and, so far, only contract of this principal investigator.
No publications have resulted from this contract so far.

Unclassified

Security Classification

DOCUMENT CONTROL DATA - R & D

(Security classification of title, body of abstract and indexing annotation must be entered when the overall report is classified)

1. ORIGINATING ACTIVITY *(Corporate author)*
University of California, San Diego
Dept.of Applied Physics & Information Science
La Jolla, California 92037

2a. REPORT SECURITY CLASSIFICATION
Unclassified

2b. GROUP

3. REPORT TITLE
OPTIMUM TECHNIQUES FOR MEASURING SPECTRAL, SPATIAL AND TEMPORAL DISTRIBUTION OF RADIATION

4. DESCRIPTIVE NOTES *(Type of report and inclusive dates)*
Scientific Final: May 1969 - June 1970 Approved 7 August 1970

5. AUTHOR(S) *(First name, middle initial, last name)*
Adolf W. Lohmann

6. REPORT DATE
30 June 70

7a. TOTAL NO. OF PAGES
39

7b. NO. OF REFS
3

8a. CONTRACT OR GRANT NO.
F 19628-69-C-0268
ARPA Order No. 1366

b. PROJECT,
8692

c. DOD ELEMENT
62301 D

d. DOD SUBELEMENT N/A

9a. ORIGINATOR'S REPORT NUMBER(S)

9b. OTHER REPORT NO(S) *(Any other numbers that may be assigned this report)*
AFCRL-70-0394

10. DISTRIBUTION STATEMENT 2-This document is subject to special export controls and each transmittal to foreign governments or foreign nationals may be made only with prior approval of AFCRL(CROO), L. G. Hanscom Field, Bedford, Massachusetts 01730

11. SUPPLEMENTARY NOTES
This research was supported by the Advanced Research Projects Agency

12. SPONSORING MILITARY ACTIVITY
Air Force Cambridge Research Laboratories (CRO)
L. G. Hanscom Field
Bedford, Massachusetts 01730

13. ABSTRACT

It is planned to send an infrared scanner in a balloon up to high altitudes. Azimuth scanning is accomplished by the torsion of the gondola. The elevation angle of the scanning telescope is incremented stepwise after each full revolution. In this report the scanning mode is studied and improvements thereof are suggested. For a follow-up instrument it is suggested that the scanning rate should not be limited by the slow torsion. In a next approach the elevation would be scanned fast compared to the torsion. Ultimately a "Multiplex Scanner" should look at many directions simultaneously. The principle of a multiplex scanner is outlined.

DD FORM 1 NOV 65 1473

Unclassified

Security Classification

14. KEY WORDS	LINK A		LINK B		LINK C	
	ROLE	WT	ROLE	WT	ROLE	WT
infrared, balloon-borne, scanning mode, multiplex scanner, Fellgett-multiplex advantage.						